Husimi distribution and phase space analysis of Dicke model quantum phase transition

E. Romera
Departamento de Física Atómica, Molecular y Nuclear and Instituto Carlos I de Física Teórica y Computacional, Universidad de Granada, Fuentenueva s/n, 18071 Granada, Spain

R. del Real
Departamento de Física Atómica, Molecular y Nuclear, Universidad de Granada, Fuentenueva s/n, 18071 Granada, Spain

M. Calixto
Departamento de Matemática Aplicada, Universidad de Granada, Fuentenueva s/n, 18071 Granada, Spain
(Dated: September 24, 2014)

The Husimi distribution is proposed for a phase space analysis of quantum phase transitions in the Dicke model of spin-boson interactions. We show that the inverse participation ratio and Wehrl entropy of the Husimi distribution give sharp signatures of the quantum phase transition. The analysis has been done using two frameworks: a numerical treatment and an analytical variational approximation. Additionally we have proposed a new characterization of the Dicke model quantum phase transition by means of the zeros of the Husimi distribution in the variational approach.

arXiv:1409.6356v1 [quant-ph] 19 Sep 2014

I. INTRODUCTION

Understanding quantum phase transitions (QPTs) is a relevant fact in quantum many body problems [1]. QPTs usually occur in a system described by a Hamiltonian of the form $H = H_0 + \lambda H_1$, with H_0 exactly solvable, H_1 an interaction term and λ the corresponding control interaction-strength parameter. The QPT occurs when λ reaches some critical value λ_c in which the symmetries (and consequently the properties) of the system change drastically. This is the case of an ensemble of atoms interacting with a single bosonic field mode described by the Dicke Hamiltonian.

Quantum mechanics offers different distributions to characterize phase-space properties [2]. One is the Wigner function, widely used in quantum optics. Other is the Husimi distribution, which is given by the overlap between a minimal uncertainty (coherent) state and the wavefunction. This distribution is sometimes more convenient because, unlike Wigner distribution, it is non-negative. Husimi distribution has been found useful for a phase-space visualization of a metal-insulator transition [3], to analyze quantum chaos in atomic physics [4] or to analyze models in condensed matter physics [5]. In addition, we would like to point out that the zeros of the Husimi distribution have essential information, in particular, the quantum state can be described by its distribution of zeros [6]. They are simply the least probable points in phase space and they have been considered as a quantum indicator of classical and quantum chaos [7, 8]

The Husimi distribution has a great amount of information and it can be useful to consider informational measures as the so-called inverse participation ratio and Wehrl entropy [9]. Recently, an analysis of QPT in the Dicke model by means of information measures [10–14] has been done in position and momentum spaces, separately. Here we will do an informational description of the Dicke model QPT in phase space in terms of the inverse participation ration (and higher moments) and the Wehrl entropy of the Husimi distribution and its marginals. Additionally we will investigate the visualization of Dicke model QPT through the zeros of the Husimi distribution.

This article is organized as follows. In Section II we briefly remind the Dicke Hamiltonian, introduce coherent states and the Husimi distribution of the ground state, define moments, Rénnyi-Wehrl entropies and marginals of the Husimi distribution and present numerical results. In Section III we study a variational approximation to the ground state wave function in terms of symmetry-adapted coherent states and analyze the information measures in the thermodynamic limit. Zeros of the Husimi (ansatz) distribution are also computed and graphically represented in order to characterize the QPT.

II. DICKE HAMILTONIAN AND HUSIMI DISTRIBUTION

The single-mode Dicke model is a well studied object in the field of QPTs [15–17]. In this case the Hamiltonian is given by

$$H = \omega_0 J_z + \omega a^\dagger a + \frac{\lambda}{\sqrt{2j}}(a^\dagger + a)(J_+ + J_-), \quad (1)$$

describing an ensemble of N two-level atoms with level-splitting ω_0, with J_z, $J_\pm$ the angular momentum operators for a pseudospin of length $j = N/2$, and a and $a^\dagger$ are the bosonic operators of the field with frequency ω. It is well known that there is a QPT at the critical value of the coupling parameter $\lambda = \lambda_c = \frac{\sqrt{\omega\omega_0}}{2}$ from the so-called normal phase ($\lambda < \lambda_c$) to the superradiant phase ($\lambda > \lambda_c$). Let us consider a basis set $\{|n; j, m\rangle \equiv |n\rangle \otimes |j, m\rangle\}$ of the Hilbert space, with

$\{|n\rangle\}_{n=0}^{\infty}$ the number states of the field and $\{|j,m\rangle\}_{m=-j}^{j}$ the so called Dicke states of the atomic sector. The matrix elements of the Hamiltonian in this basis are:

$$\begin{aligned}\langle n';j',m'|H|n;j,m\rangle &= (n\omega+m\omega_0)\delta_{n',n}\delta_{m',m}\\ &+\frac{\lambda}{\sqrt{2j}}(\sqrt{n+1}\delta_{n',n+1}+\sqrt{n}\delta_{n',n-1})\\ &\times(\sqrt{j(j+1)-m(m+1)}\delta_{m',m+1}\\ &+\sqrt{j(j+1)-m(m-1)}\delta_{m',m-1}). \end{aligned} \quad (2)$$

At this point it is important to note that time evolution preserves the parity $e^{i\pi(n+m+j)}$ of a given state $|n;j,m\rangle$. That is, the parity operator $\hat{\Pi}=e^{i\pi(a^\dagger a+J_z+j)}$ commutes with H and both operators can then be jointly diagonalized. In particular, the ground state must be even (see later on Eq. (28)).

A. Coherent states and Husimi distribution

Let us denote by

$$\begin{aligned}&|\alpha\rangle = e^{-|\alpha|^2/2}e^{\alpha a^\dagger}|0\rangle = e^{-|\alpha|^2/2}\textstyle\sum_{n=0}^{\infty}\frac{\alpha^n}{\sqrt{n!}}|n\rangle,\\ &|z\rangle = (1+|z|^2)^{-j}e^{zJ_+}|j,-j\rangle =\\ &(1+|z|^2)^{-j}\textstyle\sum_{m=-j}^{j}\binom{2j}{j+m}^{1/2}z^{j+m}|j,m\rangle,\end{aligned} \quad (3)$$

(with $\alpha,z\in\mathbb{C}$) the standard (canonical or Glauber) and spin-j Coherent States (CSs) for the photon and the particle sectors, respectively. It is well known (see e.g. [18]) that coherent states form an overcomplete set of the corresponding Hilbert space and fulfill the closure relations or resolutions of the identity:

$$\begin{aligned}1 &= \frac{1}{\pi}\int_{\mathbb{R}^2}|\alpha\rangle\langle\alpha|d^2\alpha,\\ 1 &= \frac{2j+1}{\pi}\int_{\mathbb{R}^2}|z\rangle\langle z|\frac{d^2z}{(1+|z|^2)^2},\end{aligned} \quad (4)$$

with $d^2w=d\mathrm{Re}(w)=d\mathrm{Im}(w)$ the Lebesgue measure on $\mathbb{R}^2$ or $\mathbb{C}$. It is straightforward to see that the probability amplitude of detecting n photons and $j+m$ excited atoms in $|\alpha,z\rangle\equiv|\alpha\rangle\otimes|z\rangle$ is given by:

$$\varphi_{n,m}^{(j)}(\alpha,z)=\langle n|\alpha\rangle\langle j,m|z\rangle=\frac{e^{-|\alpha|^2/2}\alpha^n}{\sqrt{n!}}\frac{\sqrt{\binom{2j}{j+m}}z^{j+m}}{(1+|z|^2)^j}. \quad (5)$$

The ground state vector ψ will be given as an expansion

$$|\psi\rangle=\sum_{n=0}^{n_c}\sum_{m=-j}^{j}c_{nm}^{(j)}|n;j,m\rangle \quad (6)$$

where the coefficients $c_{nm}^{(j)}$ are calculated by numerical diagonalization of (2) with a given cutoff n_c. The Husimi distribution of ψ is then given by

$$\begin{aligned}\Psi(\alpha,z) &= |\langle\alpha,z|\psi\rangle|^2 \quad (7)\\ &= \sum_{n,n'=0}^{n_c}\sum_{m,m'=-j}^{j}c_{nm}^{(j)}\bar{c}_{n'm'}^{(j)}\varphi_{n,m}^{(j)}(\alpha,z)\varphi_{n,m}^{(j)}(\bar{\alpha},\bar{z})\end{aligned}$$

and normalized according to:

$$\frac{2j+1}{\pi^2}\int_{\mathbb{R}^4}\Psi(\alpha,z)d^2\alpha\frac{d^2z}{(1+|z|^2)^2}=1. \quad (8)$$

Before discussing marginals of the Husimi distribution and their properties, let us introduce an important approximation which will simplify things greatly.

B. Holstein-Primakoff representation and large pseudospin

We shall make use of the Holstein-Primakoff representation [19] of the angular momentum operators $J_\pm, J_z$ in terms of the bosonic operators, $[b,b^\dagger]=1$, given by:

$$\begin{gathered}J_+=b^\dagger\sqrt{2j-b^\dagger b},\quad J_-=\sqrt{2j-b^\dagger b}\,b\\ J_z=(b^\dagger b-j).\end{gathered} \quad (9)$$

For high values of j (and fixed $b^\dagger b$), we can approximate $J_+\simeq\sqrt{2j}\,b^\dagger$ and $J_-\simeq\sqrt{2j}\,b$, so that the atomic sector can be practically described by an harmonic oscillator, just like the field sector. Introducing then position and momentum operators for the two bosonic modes as usual:

$$\begin{aligned}&X=\tfrac{1}{\sqrt{2\omega}}(a^\dagger+a),\ \ P_X=i\sqrt{\tfrac{\omega}{2}}(a^\dagger-a),\\ &Y=\tfrac{1}{\sqrt{2\omega_0}}(b^\dagger+b),\ \ P_Y=i\sqrt{\tfrac{\omega_0}{2}}(b^\dagger+b),\end{aligned} \quad (10)$$

the wave function position representation is formally equivalent to that of a set of two coupled harmonic oscillators and can be written as [20]:

$$\psi(x,y)=\sqrt{\omega\omega_0}e^{-\frac{1}{2}(\omega x^2+\omega_0y^2)}\sum_{n=0}^{n_c}\sum_{m=-j}^{j}c_{nm}^{(j)}$$

$$\times\frac{H_n(\sqrt{\omega}x)H_{j+m}(\sqrt{\omega_0}y)}{2^{(n+m+j)/2}\sqrt{n!(j+m)!}} \quad (11)$$

where we have made use of the definition of

$$\begin{aligned}\langle x|n\rangle &= \sqrt{\omega}e^{-\frac{1}{2}\omega x^2}\frac{H_n(\sqrt{\omega}x)}{\sqrt{2^n n!\sqrt{\pi}}}, \quad (12)\\ \langle y|j,m\rangle &= \sqrt{\omega_0}e^{-\frac{1}{2}\omega_0y^2}\frac{H_{j+m}(\sqrt{\omega_0}y)}{\sqrt{2^{(j+m)}(j+m)!\sqrt{\pi}}},\end{aligned}$$

(the Hermite polynomials of degree n and $j+m$, respectively) and we have truncated the Hilbert space of the field sector to dimension n_c looking for the numerical solution and convergence of the eigenproblem [21]. This is a very convenient representation that has already been used in Ref. [20]. Analogously in momentum space:

$$\tilde{\psi}(p_x,p_y)=\frac{1}{\sqrt{\omega\omega_0}}e^{-\frac{1}{2}(\frac{p_x^2}{\omega}+\frac{p_y^2}{\omega_0})}\sum_{n=0}^{n_c}\sum_{m=-j}^{j}(-i)^{n+m+j}c_{nm}^{(j)}$$

$$\times \frac{H_n(p_x/\sqrt{\omega})H_{j+m}(p_y/\sqrt{\omega_0})}{2^{(n+m+j)/2}\sqrt{n!(j+m)!}}. \quad (13)$$

Moreover, redefining

$$\beta \equiv \sqrt{2j}\, z, \quad (14)$$

in (3), it can be seen (see e.g. [18, 22]) that spin-j coherent states $|z\rangle$ go over to ordinary coherent states $|\beta\rangle \equiv e^{-|\beta|^2/2}e^{\beta b^\dagger}|0\rangle$ for $j \gg 1$ (when identifying $|j,-j\rangle \equiv |0\rangle$ and $|j,m\rangle \equiv |m+j\rangle$). Thus, we shall assume the approximation:

$$|z\rangle \simeq |\beta\rangle, \quad (15)$$

which turns out to be a quite good estimate, even for relatively small values of j, for $|z|$ in a neighborhood of the equilibrium value $|z_e| < 1$ in (27). With this approximation, the Husimi distribution (7) becomes

$$\begin{aligned}\Phi(\alpha,\beta) &= |\langle\alpha,\beta|\psi\rangle|^2 \quad (16)\\ &= \sum_{n,n'=0}^{n_c}\sum_{m,m'=-j}^{j} c^{(j)}_{nm}\bar{c}^{(j)}_{n'm'}\phi^{(j)}_{n,m}(\alpha,\beta)\phi^{(j)}_{n',m'}(\bar{\alpha},\bar{\beta}),\end{aligned}$$

where now

$$\phi^{(j)}_{n,m}(\alpha,\beta) = \langle n|\alpha\rangle\langle j+m|\beta\rangle = \frac{e^{-|\alpha|^2/2}\alpha^n}{\sqrt{n!}}\frac{e^{-|\beta|^2/2}\beta^{m+j}}{\sqrt{(m+j)!}} \quad (17)$$

with the new normalization

$$\int_{\mathbb{R}^4}\Phi(\alpha,\beta)\frac{d^2\alpha d^2\beta}{\pi^2} = 1. \quad (18)$$

C. Moments, Rényi-Wehrl entropy and marginals of the Husimi distribution

Important quantities to visualize the QPT in the Dicke model across the critical point λ_c will be the ν-th moments of the Husimi distribution (16):

$$M_{j,\nu}(\lambda) = \int_{\mathbb{R}^4}\frac{d^2\alpha d^2\beta}{\pi^2}(\Phi(\alpha,\beta))^\nu. \quad (19)$$

Note that $M_{j,1} = 1$ since Φ is normalized (18). Among all moments we shall single-out the so-called "inverse participation ratio" $P_j(\lambda) = M_{j,2}(\lambda)$ which somehow measures the (de-)localization of Φ across the phase transition. The definition of the moments $M_{j,\nu}$ is not restricted to integer values of ν. Once $M_{j,\nu}$ are known for all integer ν, there is a unique analytic extension to complex (and therefore real) ν, as integers are dense at infinity. The "classical" (versus quantum von Neumann) Rényi-Wehrl entropy is then defined as:

$$W_{j,\nu}(\lambda) = \frac{1}{1-\nu}\ln(M_{j,\nu}(\lambda)), \quad (20)$$

which tends to the Wehrl entropy

$$W_j(\lambda) = -\int_{\mathbb{R}^4}\frac{d^2\alpha d^2\beta}{\pi^2}\,\Phi(\alpha,\beta)\ln\Phi(\alpha,\beta) \quad (21)$$

when $\nu \to 1$.

In order to differentiate between position and momentum behaviors, we shall study the marginals of the Husimi distribution in each space:

$$\begin{aligned}\Phi_1(\alpha_1,\beta_1) &= \int_{\mathbb{R}^2}\frac{d\alpha_2 d\beta_2}{\pi}\Phi(\alpha_1+i\alpha_2,\beta_1+i\beta_2)\\ \Phi_2(\alpha_2,\beta_2) &= \int_{\mathbb{R}^2}\frac{d\alpha_1 d\beta_1}{\pi}\Phi(\alpha_1+i\alpha_2;\beta_1+i\beta_2), \quad (22)\end{aligned}$$

so that

$$\int_{\mathbb{R}^2}\frac{d\alpha_\kappa d\beta_\kappa}{\pi}\Phi_\kappa(\alpha_\kappa,\beta_\kappa) = 1,\ \kappa = 1,2. \quad (23)$$

We shall also be interested in the moments of marginal distributions

$$M^{(\kappa)}_{j,\nu}(\lambda) = \int_{\mathbb{R}^2}\frac{d\alpha_\kappa d\beta_\kappa}{\pi}(\Phi_\kappa(\alpha_\kappa,\beta_\kappa))^\nu,\ \kappa = 1,2, \quad (24)$$

specially the marginal inverse participation ratios $P^{(\kappa)}_j(\lambda) = M^{(\kappa)}_{j,2}$ and marginal Wehrl entropies

$$W^{(\kappa)}_j(\lambda) = -\int_{\mathbb{R}^2}\frac{d\alpha_\kappa d\beta_\kappa}{\pi}\,\Phi_\kappa(\alpha_\kappa,\beta_\kappa)\ln\Phi_\kappa(\alpha_\kappa,\beta_\kappa) \quad (25)$$

in position ($\kappa = 1$) and momentum ($\kappa = 2$) spaces as a function of the control parameter λ. In general, $P_j(\lambda) \neq P^{(1)}_j(\lambda)P^{(2)}_j(\lambda)$ and $W_j(\lambda) \neq W^{(1)}_j(\lambda)+W^{(2)}_j(\lambda)$, but these quantities are approximately equal for high j except in a close neighborhood of λ_c [3].

In Appendix A we provide a connection with other phase-space formulas for marginal distributions in position and momentum coordinates (10). This approach has been used in [3] to visualize the metal-insulator QPT described by the Aubry-André model. We also make use of this representation to make numerical calculations more maneuverable.

D. Numerical Results

Firstly we have calculated the participation ratio $P_j(\lambda)$ and the Wherl entropy $W_j(\lambda)$ for different values of λ. The computed results are given in Fig. 1 where we present $P_j(\lambda)$ and $W_j(\lambda)$ for $j = 2, 5, 10$ and for $\omega = \omega_0 = 1$ (for which $\lambda_c = 0.5$). Notice that the inverse partipation ratio (top pannel) is around $1/4$ in the normal phase decreasing around the critical point to reach the value $1/8$ in the superradiant phase. We can see that the change in the participation ratio is suddener as j increases. The Wherl entropy (botton panel) is approximately 2 in the normal phase and around $2 + \ln 2$ in the superradiant phase changing suddenly (suddener as j increases) around the critical point. For completeness we have represented the computed marginal quantities in figure 2.

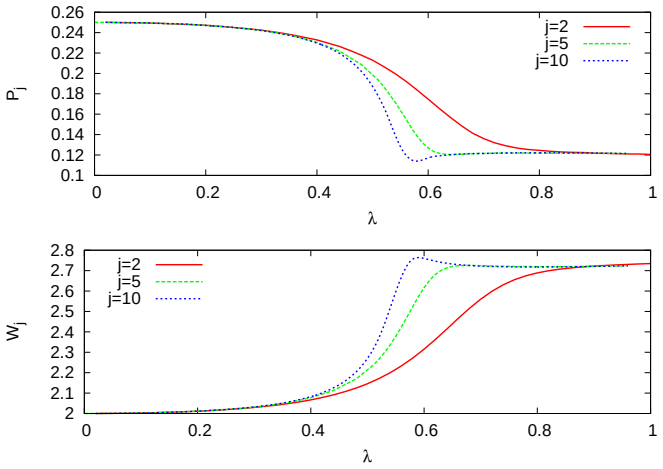

FIG. 1: Inverse participation ratio $P_j(\lambda)$ and entropy in phase space $W_j(\lambda)$ for $j = 5$ and $j = 10$ and $\omega_0 = \omega = 1$ as a function of λ

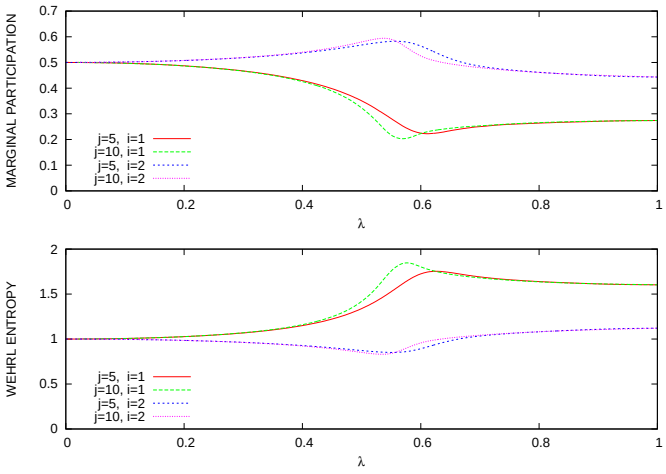

FIG. 2: Inverse participation ratio $P_j^{(i)}\lambda)$ and entropy in phase space $W_j^{(i)}(\lambda)$ for $j = 5$ and $j = 10$, $i = 1$, 2 and $\omega_0 = \omega = 1$ as a function of λ

III. VARIATIONAL APROXIMATION AND THE THERMODYNAMIC LIMIT

Now we present analytical expressions for Husimi's distribution, its marginals, moments and entropies using trial states expressed in terms of "parity-symmetry-adapted" CSs introduced by Castaños et al. [23, 24], which turn out to be an excellent approximation to the exact quantum solution of the ground (+) and first excited (−) states of the Dicke model.

A. Symmetry-adapted coherent states and their Husimi distribution

Using the direct product $|\alpha, z\rangle \equiv |\alpha\rangle \otimes |z\rangle$ as a ground-state ansatz, one can easily compute the mean energy

$$\begin{aligned}\mathcal{H}(\alpha, z) &= \langle \alpha, z|H|\alpha, z\rangle \\ &= \omega|\alpha|^2 + j\omega_0 \tfrac{|z|^2-1}{|z|^2+1} + \lambda\sqrt{2j}(\alpha+\bar{\alpha})\tfrac{\bar{z}+z}{|z|^2+1},\end{aligned} \tag{26}$$

which defines a four-dimensional "energy surface". Minimizing with respect to these four coordinates gives the equilibrium points:

$$\begin{aligned}\alpha_e &= \begin{cases} 0, & \text{if } \lambda < \lambda_c \\ -\sqrt{2j}\sqrt{\frac{\omega_0}{\omega}}\frac{\lambda}{\lambda_c}\sqrt{1-\left(\frac{\lambda}{\lambda_c}\right)^{-4}}, & \text{if } \lambda \geq \lambda_c \end{cases} \\ z_e &= \begin{cases} 0, & \text{if } \lambda < \lambda_c \\ \sqrt{\frac{\frac{\lambda}{\lambda_c}-\left(\frac{\lambda}{\lambda_c}\right)^{-1}}{\frac{\lambda}{\lambda_c}+\left(\frac{\lambda}{\lambda_c}\right)^{-1}}}, & \text{if } \lambda \geq \lambda_c \end{cases}\end{aligned} \tag{27}$$

Note that α_e and z_e are real and non-zero above the critical point λ_c (i.e., in the superradiant phase).

Although the direct product $|\alpha, z\rangle$ gives a good variational approximation to the ground state mean energy in the thermodynamic limit $j \to \infty$, it does not capture the correct behavior for other ground state properties sensitive to the parity symmetry $\hat{\Pi}$ of the Hamiltonian (1) like, for instance, uncertainty and entropy measures. This is why parity-symmetry adapted coherent states are introduced. Indeed, a far better variational description of the ground (resp. first-excited) state is given in terms of the even-(resp. odd)-parity coherent states

$$|\psi_\pm\rangle = |\alpha, z, \pm\rangle = \frac{|\alpha\rangle \otimes |z\rangle \pm |-\alpha\rangle \otimes |-z\rangle}{\mathcal{N}_\pm(\alpha, z)}, \tag{28}$$

obtained by applying projectors of even and odd parity $\hat{\mathcal{P}}_\pm = (1 \pm \hat{\Pi})$ to the direct product $|\alpha\rangle \otimes |z\rangle$. Here

$$\mathcal{N}_\pm(\alpha, z) = \sqrt{2}\left(1 \pm e^{-2|\alpha|^2}\left(\frac{1-|z|^2}{1+|z|^2}\right)^{2j}\right)^{1/2} \tag{29}$$

is a normalization factor. These even and odd coherent states are "Schrodinger's cat states" in the sense that they are a quantum superposition of quasi-classical, macroscopically distinguishable states. The new energy surface is now:

$$\begin{aligned}\mathcal{H}_\pm(\alpha, z) &= \langle \alpha, z, \pm|H|\alpha, z, \pm\rangle \\ &= \frac{\mathcal{H}(\alpha, z) \pm \langle \alpha, z|H|-\alpha, -z\rangle}{\mathcal{N}_\pm^2(\alpha, z)/2},\end{aligned} \tag{30}$$

with non-diagonal elements

$$\begin{aligned}\langle \alpha, z|H|-\alpha, -z\rangle = e^{-2|\alpha|^2}\left(\frac{1-|z|^2}{1+|z|^2}\right)^{2j} \times \\ \left(\omega|\alpha|^2 - j\omega_0\frac{1+|z|^2}{1-|z|^2} + \lambda\sqrt{2j}(\alpha-\bar{\alpha})\frac{z-\bar{z}}{1-|z|^2}\right)\end{aligned} \tag{31}$$

The more involved structure of $\mathcal{H}_{\pm}(\alpha, z)$ makes much more difficult to obtain the new critical points $\alpha_e^{(\pm)}, z_e^{(\pm)}$ minimizing the corresponding energy surface. Instead of carrying out a numerical computation of $\alpha_e^{(\pm)}, z_e^{(\pm)}$ for different values of j and λ, we shall use the approximation $\alpha_e^{(\pm)} \approx \alpha_e, z_e^{(\pm)} \approx z_e$, which turns out to be quite good except in a close neighborhood around λ_c which diminishes as the number of particles $N = 2j$ increases (see Ref. [24]). With this approximation, we expect a rather good agreement between our numerical and variational results except perhaps in a close vicinity of λ_c.

Taking into account the coherent state overlaps

$$\begin{aligned} \langle \alpha | \pm \alpha_e \rangle &= e^{-\frac{1}{2}|\alpha| - \frac{1}{2}\alpha_e^2 \pm \bar{\alpha}\alpha_e}, \\ \langle z | \pm z_e \rangle &= \frac{(1 \pm \bar{z} z_e)^{2j}}{(1+|z|^2)^j (1+z_e^2)^j}, \end{aligned} \tag{32}$$

the Husimi distribution for the variational states $|\alpha_e, z_e, \pm\rangle$ can be simply written as:

$$\Psi_{\pm}(\alpha, z) = \frac{|\langle \alpha, z | \alpha_e, z_e \rangle \pm \langle \alpha, z | -\alpha_e, -z_e \rangle|^2}{\mathcal{N}_{\pm}^2(\alpha_e, z_e)}. \tag{33}$$

In order to compute the zeros, moments and entropies of $\Psi_{\pm}(\alpha, z)$, and to compare with numerical results of the previous section, we shall make use of the Holstein-Primakoff representation (9,14,15). With this approximation, the Husimi distribution can be cast in the new form

$$\Phi_{\pm}(\alpha, \beta) = \frac{e^{-|\alpha|^2 - |\beta|^2 - \alpha_e^2 - \beta_e^2} |e^{\bar{\alpha}\alpha_e + \bar{\beta}\beta_e} \pm e^{-\bar{\alpha}\alpha_e - \bar{\beta}\beta_e}|^2}{2\left(1 \pm e^{-2\alpha_e^2 - 2\beta_e^2}\right)}, \tag{34}$$

From now on we shall restrict ourselves to the even case and simply denote by $\psi = \psi_+$ and $\Phi = \Phi_+$ the wave function and the Husimi distribution of the variational ground state.

B. Moments and Rényi-Wehrl entropy of the Husimi distribution

Important quantities to visualize the QPT in the Dicke model accross the critical point λ_c will be the νth moments of the Husimi distrubution (19). In particular, the inverse participation ratio is given by

$$P_j(\lambda) = M_{j,2}(\lambda) = \frac{1 + \operatorname{sech}^2(\alpha_e^2 + \beta_e^2)}{8} \tag{35}$$

Figure 3 shows that $P_j(\lambda)$ tends to a Heaviside-type step function

$$P_{\infty}(\lambda) = \begin{cases} 1/4, & \text{if } \lambda < \lambda_c \\ 1/8, & \text{if } \lambda \geq \lambda_c, \end{cases} \tag{36}$$

which suffers a sudden decrease of 1/4 from normal to superradiant phase, thus indicating a delocalization of Φ

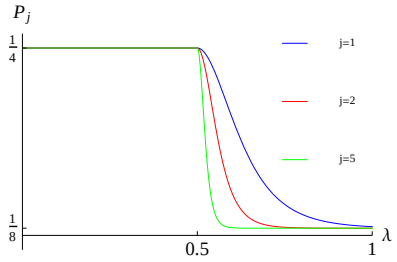

FIG. 3: Inverse participation ratio of the Husimi distribution as a function of λ for different values of j and $\lambda_c = 0.5$.

above the critical point λ_c. A similar behavior is displayed by higher moments in the thermodynamic limit

$$M_{j,\nu}(\lambda) \overset{j\to\infty}{\longrightarrow} \begin{cases} \nu^{-2}, & \text{if } \lambda < \lambda_c \\ 2^{1-\nu}\nu^{-2}, & \text{if } \lambda \geq \lambda_c. \end{cases} \tag{37}$$

The definition of the moments $M_{j,\nu}$ is not restricted to integer values of ν. Once $M_{j,\nu}$ are known for all integer ν, there is a unique analytic extension to real $\nu > 0$ (and to the right half complex plane). This analytic extension is possible due to the particular expression of Φ in therms of Gaussian bells. Using (37), we can easily compute Rényi-Wehrl entropies (20) and, in the limit $\nu \to 1$, the Wehrl entropy (21) in the thermodynamic limit

$$W_j(\lambda) \overset{j\to\infty}{\longrightarrow} \begin{cases} 2, & \text{if } \lambda < \lambda_c \\ 2 + \ln(2), & \text{if } \lambda \geq \lambda_c. \end{cases} \tag{38}$$

This result is in agreement with the (still unproved) Lieb's conjecture. Indeed, as conjectured by Wehrl [25] and proved by Lieb [26], any Glauber coherent state $|\alpha\rangle$ has a minimum Wehrl entropy of 1. In the same paper by Lieb [26], it was also conjectured that the extension of Wehrl's definition of entropy for coherent spin-j states will yield a minimum entropy $j/(j+1)$. For the joined system of radiation field plus atoms we would have $W_j(\lambda) = 1 + j/(j+1)$ in the normal phase ($\lambda < \lambda_c$), and therefore, $W_j \to 2$ in the thermodynamic limit, in agreement with our result.

C. Marginals of the Husimi distribution

The explicit expression of the marginal Husimi distributions (22) for our variational ground state ψ are

$$\begin{aligned} \Phi_1(\alpha_1, \beta_1) &= \frac{1 + e^{\alpha_e^2 + \beta_e^2} \cosh(2(\alpha_1\alpha_e + \beta_1\beta_e))}{e^{\alpha_1^2 + \beta_1^2}(1 + e^{2\alpha_e^2 + 2\beta_e^2})}, \\ \Phi_2(\alpha_2, \beta_2) &= \frac{1 + e^{-\alpha_e^2 - \beta_e^2} \cos(2(\alpha_2\alpha_e + \beta_2\beta_e))}{e^{\alpha_2^2 + \beta_2^2}(1 + e^{-2\alpha_e^2 - 2\beta_e^2})}. \end{aligned} \tag{39}$$

Using the definition (24), we can compute inverse participation ratios for marginal distributions as a function

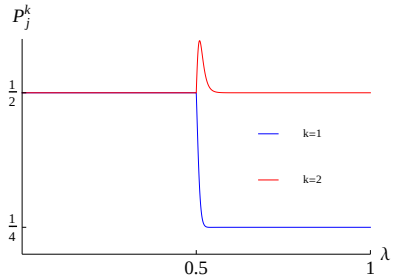

FIG. 4: Marginal inverse participation ratios $P_j^{(\kappa)}, \kappa = 1, 2$ (position and momentum, resp.) of the Husimi distribution as a function of λ for $j = 10$ and $\lambda_c = 0.5$.

of $\zeta_j(\lambda) \equiv e^{\alpha_e^2+\beta_e^2}$:

$$P_j^{(1)}(\lambda) = \frac{2+4\zeta_j^{3/2}(\lambda)+\zeta_j^2(\lambda)+\zeta_j^4(\lambda)}{4(1+\zeta_j^2(\lambda))^2},$$
$$P_j^{(2)}(\lambda) = \frac{1+\zeta_j^2(\lambda)+4\zeta_j^{5/2}(\lambda)+2\zeta_j^4(\lambda)}{4(1+\zeta_j^2(\lambda))^2}. \quad (40)$$

Figure 4 shows $P_j^{(\kappa)}(\lambda)$ for $j = 10$, indicating that $P_j^{(1)}(\lambda)$ suffers a sudden decrease from 1/2 to 1/4 across the phase transition, whereas $P_j^{(2)}(\lambda)$ remains constant (the small peak around $\lambda_c = 0.5$ is perhaps an artifact due to the approximate character of α_e, β_e in a neighborhood of λ_c). In general, higher moments of marginal distributions in the thermodynamic limit are given by:

$$M_{j,\nu}^{(1)}(\lambda) \overset{j\to\infty}{\longrightarrow} \begin{cases} \nu^{-1}, & \text{if } \lambda < \lambda_c \\ 2^{1-\nu}\nu^{-1}, & \text{if } \lambda \geq \lambda_c. \end{cases},$$
$$M_{j,\nu}^{(2)}(\lambda) \overset{j\to\infty}{\longrightarrow} \nu^{-1}, \ \forall\lambda, \quad (41)$$

so that, in this limit, we have $M_{j,\nu}(\lambda) = M_{j,\nu}^{(1)}(\lambda)M_{j,\nu}^{(2)}(\lambda)$. This equality is not true in general for finite j and $\lambda > \lambda_c$, as can be directly checked for $\nu = 2$ from (35) and (40). Now we see that the entropy excess of ln(2) comes from the position contribution, since Wehrl entropy in momentum space remains constant:

$$W_j^{(1)}(\lambda) \overset{j\to\infty}{\longrightarrow} \begin{cases} 1, & \text{if } \lambda < \lambda_c \\ 1+\ln(2), & \text{if } \lambda \geq \lambda_c. \end{cases} \quad (42)$$

$$W_j^{(2)}(\lambda) \overset{j\to\infty}{\longrightarrow} 1 \quad (43)$$

In order to connect with (A3), we introduce position and momentum operators for the two bosonic modes as in (10). Taking into account the position and momentum representation of an ordinary (canonical) CS (A2), the explicit expression of the ground state wave function $|\alpha_e, \beta_e\rangle_+$ in position ($\psi(x, y) = \langle x, y|\alpha_e, \beta_e, +\rangle$) and momentum ($\tilde{\psi}(p_x, p_y) = \langle p_x, p_y|\alpha_e, \beta_e, +\rangle$) representations can be easily obtained as:

$$\psi(x,y) = \sqrt{\frac{\omega\omega_0}{\pi}}\mathcal{N}_+(\alpha_e,\beta_e) \times \left(e^{-\frac{1}{2}(\sqrt{\omega}\,x-\sqrt{2}\,\alpha_e)^2-\frac{1}{2}(\sqrt{\omega_0}\,y-\sqrt{2}\,\beta_e)^2} + e^{-\frac{1}{2}(\sqrt{\omega}\,x+\sqrt{2}\,\alpha_e)^2-\frac{1}{2}(\sqrt{\omega_0}\,y+\sqrt{2}\,\beta_e)^2}\right), \quad (44)$$

$$\tilde{\psi}(p_x,p_y) = \frac{2}{\sqrt{\omega\omega_0\pi}}\mathcal{N}_+(\alpha_e,\beta_e) \times e^{-\frac{p_x^2}{2\omega}-\frac{p_y^2}{2\omega_0}}\cos\left(\sqrt{2}(\frac{p_x}{\sqrt{\omega}}\alpha_e+\frac{p_y}{\sqrt{\omega_0}}\beta_e)\right), \quad (45)$$

where $\mathcal{N}_+(\alpha_e, \beta_e) = \left(2(1+e^{-2\alpha_e^2-2\beta_e^2})\right)^{-1/2}$ is the typical normalization factor obtained earlier. Note that for $\lambda > \lambda_c$ the ground-state wave function $\psi(x, y)$ splits up into two Gaussian packets centered at antipodal points $\sqrt{2}(\alpha_e, \beta_e)$ and $-\sqrt{2}(\alpha_e, \beta_e)$ in the $x-y$ plane. The packets move away from each other for increasing j above the critical point $\lambda > \lambda_c$. In momentum space, $\tilde{\psi}(p_x, p_y)$ is a Gaussian modulated by a cosine function which oscillates rapidly for high j for $\lambda > \lambda_c$.

D. Zeros of the Husimi distribution and QPT

It is well known that the Husimi density is determined by its zeros through the Weierstrass-Hadamard factorization. It has also been observed that the distribution of zeros differs for classically regular or chaotic systems and can be considered as a quantum indicator of classical chaos (see e.g. [4, 6, 7]).

Here we shall explore the distribution of zeros of the Husimi density as a fingerprint of QPT in the Dicke model. From (33) we obtain

$$\Psi(\alpha, z) = 0 \Rightarrow 2\bar{\alpha}\alpha_e + 2j\ln\frac{1+\bar{z}z_e}{1-\bar{z}z_e} = i\pi(2l+1),\ l \in \mathbb{Z}. \quad (46)$$

Instead of this condition, we shall use the approximation (15) and from (34) obtain

$$\Phi(\alpha, \beta) = 0 \Rightarrow 2\bar{\alpha}\alpha_e + 2\bar{\beta}\beta_e = i\pi(2l+1),\ l \in \mathbb{Z}, \quad (47)$$

which is equivalent to

$$\alpha_1 = -\frac{\beta_e}{\alpha_e}\beta_1, \quad (48)$$
$$\alpha_2 = -\frac{\beta_e}{\alpha_e}\beta_2 - \frac{\pi}{2\alpha_e}(2l+1). \quad (49)$$

We see that, in the normal phase ($\alpha_e = 0 = \beta_e$) the Husimi distribution $\Phi(\alpha, \beta)$ has no zeros. In the superradiant phase ($\lambda > \lambda_c$) the zeros are localized along straight lines ("dark fringes") in the $\alpha_1\beta_1$ (position) and $\alpha_2\beta_2$ (momentum) planes. In the momentum plane, the

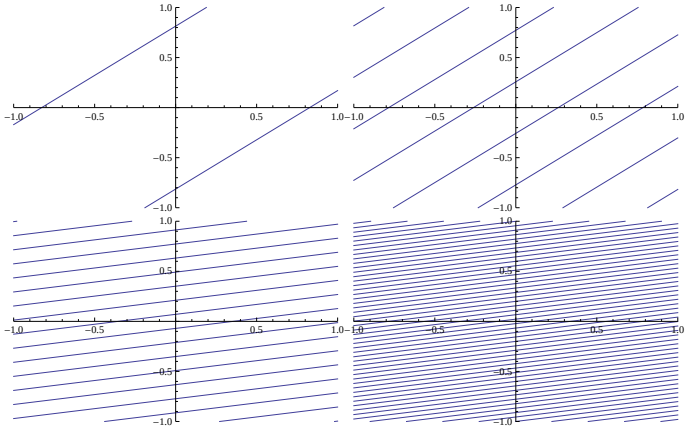

FIG. 5: Zeros of the Husimi distribution $\Phi(\alpha,\beta)$ in the cell $\alpha_2,\beta_2 \in [-1,1]$ of the momentum plane for $\lambda = 0.6, j = 10$ (top-left), $\lambda = 0.6, j = 100$ (top-right), $\lambda = 10, j = 10$ (bottom-left) and $\lambda = 10, j = 100$ (bottom-right) for $\lambda_c = 0.5$.

number of dark fringes per cell $\alpha_2,\beta_2 \in [-1,1]$ grows with λ and j, as depicted in Figure 5. In the thermodynamic limit $j \to \infty$, zeros densely fill the momentum plane $\alpha_2\beta_2$.

IV. CONCLUSIONS

We have found that inverse participation ratios and Rényi-Wehrl entropies of the Husimi distribution provide sharp indicators of a quantum phase transition in the Dicke model. This uncertainty measures detect a delocalization of the Husimi distribution across the critical point λ_c and we have employed them to quantify the phase-space spreading of the states. The advantage of working in phase space is that we can analyze contributions in position and momentum space jointly and separately. Marginal magnitudes in position space turn out to provide sharper indicators of the QPT than in momentum space, where these quantities remain nearly constant. However, zeros of the Husimi distribution exhibit a richer structure in momentum than in position space.

Calculations have been done numerically and through a variational approximation. Numerical calculations are performed by using explicit expressions which have been derived by adopting a truncation of the Holstein-Primakoff representation of the angular momentum operators. The variational approach, in terms of symmetry-adapted coherent states, complements and enriches the analysis providing explicit analytical expressions for the inverse participation ratios and Rényi-Wehrl entropies which remarkably coincide with the numerical results, especially in the thermodynamic limit.

In the superradiant phase, Wehrl's entropy undergoes an entropy excess (or "subentropy" [27]) of $\ln(2)$. This fact implies that the Husimi distribution splits up into two identical subpackets with negligible overlap in passing from normal to superradiant phase. In general, for s identical subpackets with negligible overlap, one would expect an entropy excess of $\ln(s)$. We would like to mention that the Wehrl subentropy (or excess of the Wehrl entropy) has been also used in [9] as a measure of the degree of mixing for monopartite states or of the degree of entanglement for pure states of bipartite systems. Dicke model is also known to exhibit entanglement between the atoms and the field [15, 16] and a characterization of it in terms of entropy excesses of this kind would be interesting.

The QPT fingerprints in the Dicke model have also been tracked by exploring the distribution of zeros of the Husimi density within the analytical variational approximation. We have found that the zeros characterize the QPT in this model. Moreover, zeros densely fill the momentum plane in the superradiant phase for the ground state variational approximation in the thermodynamic limit. This subject deserves further attention and should be studied in other models too. For the moment, we have detected a sudden growth of zeros above the critical point λ_c in the Holstein-Primakoff approximation.

Acknowledgments

This work was supported by the Projects: FIS2011-24149 and FIS2011-29813-C02-01 (Spanish MICINN), FQM-165/0207 and FQM219 (Junta de Andalucía).

Appendix A: Marginal Husimi distributions as Gaussian smearings

Working on resonance $\omega = \omega_0$, we can introduce a "natural variance" $\sigma^2 = 1/(2\omega)$ in the Dicke model by considering the change of coordinates

$$\begin{array}{ll} \alpha_1 = \frac{x}{2\sigma}, & \alpha_2 = \sigma k_x, \\ \beta_1 = \frac{y}{2\sigma}, & \beta_2 = \sigma k_y, \end{array} \tag{A1}$$

with $\mathbf{r} = (x,y), \mathbf{k} = (k_x,k_y)$ position and momentum vectors. Taking into account the position and momentum representation of an ordinary (canonical) CS [18]:

$$\begin{aligned} \langle x|\alpha\rangle &= \left(\frac{\omega^2}{\pi}\right)^{1/4} e^{i\sqrt{2\omega}\,\alpha_2 x} e^{-(\sqrt{\omega}\,x-\sqrt{2}\,\alpha_1)^2/2}, \\ \langle k|\alpha\rangle &= \left(\frac{1}{\pi\omega^2}\right)^{1/4} e^{i\sqrt{\frac{2}{\omega}}\,\alpha_1 k} e^{-(\frac{k}{\sqrt{\omega}}-\sqrt{2}\,\alpha_2)^2/2}, \end{aligned} \tag{A2}$$

one can easily see that marginal distributions (22) can be also obtained as a smearing (convolution product) of the density functions $|\psi(\mathbf{r})|^2$ and $|\tilde{\psi}(\mathbf{k})|^2$ by Gaussians $g_\sigma(\mathbf{r}) = (2\pi\sigma^2)^{-1}\exp\left(-\mathbf{r}^2/(2\sigma^2)\right)$ and $\tilde{g}_\sigma(\mathbf{k}) =$

$4\pi\sigma^2 \exp\left(-2\sigma^2\mathbf{k}^2\right)$ as:

$$\begin{aligned} \xi(\mathbf{r}) &= \int d\mathbf{r}' g_\sigma(\mathbf{r}-\mathbf{r}')|\psi(\mathbf{r}')|^2 \\ \tilde{\xi}(\mathbf{k}) &= \int \frac{d\mathbf{k}'}{(2\pi)^2}\tilde{g}_\sigma(\mathbf{k}-\mathbf{k}')|\tilde{\psi}(\mathbf{k}')|^2 \end{aligned} \tag{A3}$$

with $\int d\mathbf{r}\xi(\mathbf{r}) = 1$ and $\int \frac{d\mathbf{k}}{(2\pi)^2}\tilde{\xi}(\mathbf{k}) = 1$. Inverse participation ratios and and Wehrl entropies for these marginal distributions are now written as:

$$P_j^{\xi} = \int d\mathbf{r}\xi^2(\mathbf{r}), \quad P_j^{\tilde{\xi}} = \int \frac{d\mathbf{k}}{(2\pi)^2}\tilde{\xi}^2(\mathbf{k}) \tag{A4}$$

$$W_j^{\xi} = \int d\mathbf{r}\xi(\mathbf{r})\ln\xi(\mathbf{r}), \quad W_j^{\tilde{\xi}} = \int \frac{d\mathbf{k}}{(2\pi)^2}\tilde{\xi}(\mathbf{k})\ln\tilde{\xi}(\mathbf{k}). \tag{A5}$$

More, explicitly, from (11) and (13), marginal Husimi distributions (A3) are given in terms of the coefficients $c_{nm}^{(j)}$ as:

$$\xi(x,y) = \sum_{n,m,n',m'} c_{nm}^{(j)} c_{n'm'}^{(j)} I_{n,n'}(x) I_{m+j,m'+j}(y) \tag{A6}$$

and

$$\tilde{\xi}(k_x,k_y) = (2\pi)^2 \sum_{n,m,n',m'} d_{nm}^{(j)} d_{n'm'}^{(j)} I_{n,n'}(p_x) I_{m+j,m'+j}(p_y) \tag{A7}$$

with $d_{nm}^{(j)} \equiv (-i)^{n+m+j} c_{nm}^{(j)}$ and

$$\begin{aligned} I_{n,n'}(x) &= A\alpha\sqrt{n!n'!\left(\frac{1-\alpha^2}{2}\right)^{n+n'}} e^{\frac{-x^2}{1+2\sigma^2}} \\ &\times \sum_{k=0}^{\mu} B(n,n',k)\left(\frac{2}{1-\alpha^2}\right)^k H_{n+n'-2k}\left(\frac{\alpha s}{(1-\alpha^2)^{1/2}}\right) \end{aligned} \tag{A8}$$

with $\mu = \min\{n,n'\}$, $A = (2\pi\sigma^2)^{-1/2}$, $B(n,n',k) = \frac{1}{(k!)(n-k)!(n'-k)!}$, $\alpha = \sqrt{\frac{2\sigma^2}{2\sigma^2+1}}$ and $s = \frac{x}{\sigma\sqrt{2(1+2\sigma^2)}}$. Relations between marginal inverse participation ratios and Wehrl entropies in both cases can be straightforwardly obtained: $P_j^{\xi} = \pi^{-1}P_j^{(1)}$ and $P_j^{\tilde{\xi}} = \pi P_j^{(2)}$ and $W_j^{\xi} = W_j^{(1)} + \ln(2\pi)$ and $W_j^{\tilde{\xi}} = W_j^{(2)} - \ln(2\pi)$.

[1] S. Sachdev, *Quantum Phase Transitions*, Cambridge University Press (2000).
[2] C. C. Gerry and P. L. Knight, *Introductory Quantum Optics*, Cambridge University Press (2005).
[3] C. Aulbach, A. Wobst, G.-L. Ingold, P. Hanggi and I. Varga, New J. of Physics **6**, 70 (2004).
[4] P. A. Dando and T. S. Monteiro, J. Phys. B. **27**, 2681, (1994).
[5] D. Weinmann , S. Kohler, G-L. Ingold and P. Hnggi, Ann. Phys. (Lpz) 8 SI277 (1999).
[6] H. J. Korsch, C. Müller and H. Wiescher, J. Phys. A **30**, L677 (1997).
[7] P. Leboeuf and A. Voros, J. Phys. A **23**, 1765 (1990).
[8] P. A. Dando, and T. S. Monteiro, J. Phys. B **27**, 2681 (1994).
[9] F. Mintert and K. Zyczkowski, Phys. Rev. A **69**, 022317 (2004).
[10] E. Romera and Á. Nagy, Phys. Lett. A **375** 3066 (2011).
[11] E. Romera, K. Sen and Á. Nagy, J.Stat. Mech. doi:10.1088/1742-5468/2011/09/P09016
[12] E. Romera, M. Calixto and Á. Nagy, Europhys. Lett. **97**, 20011 (2012).
[13] Á. Nagy and E. Romera, Physica A doi: 10.1016/j.physa.2012.02.024 (2012).
[14] M. Calixto, Á. Nagy, I. Paraleda and E. Romera (submitted, 2012).
[15] N. Lambert, C. Emary, and T. Brandes, Phys. Rev. Lett. **92**, 073602 (2004).
[16] N. Lambert, C. Emary, and T. Brandes, Phys. Rev.A **71**, 053804 (2005).
[17] T. Brandes, Phys. Rep. **408**, 315 (2005).
[18] A. Perelomov, Generalized Coherent States and Their Applications, Springer-Verlag (1986).
[19] T. Holstein and H. Primakoff, Phys. Rev. **58**, 1098 (1940).
[20] C. Emary and T. Brandes, Phys. Rev. E **67**, 066203 (2003).
[21] M. A. Bastarrachea-Magnani, J. G. Hirsch *Numerical solutions of the Dicke Hamiltonian*, arXiv:1108.0703 (2011)
[22] J.M. Radcliffe, J. Phys. A **4**, 313 (1971).
[23] O. Castaños, E. Nahmad-Achar, R. López-Peña and J. G. Hirsch, Phys. Rev. A **83**, 051601 (2011).
[24] O. Castaños, E. Nahmad-Achar, R. López-Peña, and J. G. Hirsch, Phys. Rev. A, **84** 013819 (2011).
[25] A. Wehrl, Rep. Math. Phys. **16**, 353 (1979)
[26] E.H. Lieb, Commun. Math. Phys. **62**, 35 (1978)
[27] R. Jozsa, D. Robb and W.K. Wootters, Phys. Rev. A **49**, 668 (1994).